Pathogen lifestyle determines host genetic signature of quantitative disease resistance loci in oilseed rape (*Brassica napus*)

Catherine N. Jacott[1], Henk-jan Schoonbeek[1], Gurpinder Singh Sidhu[2], Burkhard Steuernagel[2], Rachel Kirby[1], Xiaorong Zheng[3], Andreas von Tiedermann[3], Violetta K. Macioszek[4], Andrzej K. Kononowicz[5], Heather Fell[6], Bruce D.L. Fitt[6], Georgia K. Mitrousia[6,7], Henrik U. Stotz[6], Christopher J. Ridout[1], Rachel Wells[1]

[1] Crop Genetics Department, John Innes Centre, Norwich Research Park, Norwich, NR4 7UH, UK

[2] Computational and Systems Biology Department, John Innes Centre, Norwich Research Park, Norwich, NR4 7UH, UK

[3] Department of Crop Sciences, Georg August University, Göttingen, Germany

[4] Department of Biology and Plant Ecology, Faculty of Biology, University of Bialystok, 15-245 Bialystok, Poland

[5] Department of Plant Ecophysiology, Faculty of Biology and Environmental Protection, University of Lodz, 90-237 Lodz, Poland

[6] Centre for Agriculture, Food and Environmental Management Research, School of Life and Medical Sciences, University of Hertfordshire, Hatfield, Hertfordshire AL10 9AB, UK

[7] Rothamsted Research, Harpenden, Hertfordshire, AL5 2JQ, UK

Authors for correspondence: Rachel Wells

Email: rachel.wells@jic.ac.uk

ORCiDs

Catherine N. Jacott	http://orcid.org/0000-0002-4285-0228
Henk-jan Schoonbeek	http://orcid.org/0000-0002-1087-2553
Gurpinder Singh Sidhu	https://orcid.org/0009-0002-7905-8055
Burkhard Steuernagel	http://orcid.org/0000-0002-8284-7728
Rachel Kirby	NA
Xiaorong Zheng	http://orcid.org/0000-0002-1369-8669
Andreas von Tiedermann	http://orcid.org/0000-0002-1085-9607
Violetta K. Macioszek	http://orcid.org/0000-0002-5143-4226
Andrzej K. Kononowicz	http://orcid.org/0000-0001-9950-5102
Heather Fell	NA
Bruce D.L. Fitt	http://orcid.org/0000-0003-3981-6456
Georgia K. Mitrousia	http://orcid.org/0000-0002-5960-6555
Henrik U Stotz	http://orcid.org/0000-0003-2954-8566
Christopher J. Ridout	http://orcid.org/0000-0001-9287-938X
Rachel Wells	http://orcid.org/0000-0002-1280-7472

Total word count: 6110 words

Summary: 176 words

Introduction: 1097 words

Materials and Methods: 1421 words

Results: 2466 words, 6 tables, 3 figures (colour), 8 supporting tables, 2 supporting figures (colour)

Discussion: 1126 words

Summary

- Crops are affected by several pathogens, but these are rarely studied in parallel to identify common and unique genetic factors controlling diseases. Broad-spectrum quantitative disease resistance (QDR) is desirable for crop breeding as it confers resistance to several pathogen species.
- Here, we use associative transcriptomics (AT) to identify candidate gene loci associated with *Brassica napus* QDR to four contrasting fungal pathogens: *Alternaria brassicicola*, *Botrytis cinerea*, *Pyrenopeziza brassicae* and *Verticillium longisporum.*
- We did not identify any loci associated with broad-spectrum QDR to fungal pathogens with contrasting lifestyles. Instead, we observed QDR dependent on the lifestyle of the pathogen—hemibiotrophic and necrotrophic pathogens had distinct QDR responses and associated loci, including some loci associated with early immunity. Furthermore, we identify a genomic deletion associated with resistance to *V. longisporum* and potentially broad-spectrum QDR.
- This is the first time AT has been used for several pathosystems simultaneously to identify host genetic loci involved in broad-spectrum QDR.
- We highlight candidate loci for broad-spectrum QDR with no antagonistic effects on susceptibility to the other pathogens studies as candidates for crop breeding.

Introduction

Crop-infecting fungi are responsible for approximately 20% of global crop losses annually (Fisher *et al.*, 2018). Developing broad-spectrum resistance is vital for effective crop disease management, as it protects against several pathogen species or most races or isolates of the same pathogen (Kou and Wang, 2010). Despite this, plant interactions with different pathogens are rarely studied in collaborative programs to identify common and unique genetic factors controlling the diseases.

Most research and breeding focus on *'R'* (resistance) gene-mediated qualitative resistance, often providing complete resistance to certain races of a pathogen (McDowell and Woffenden, 2003). *R* gene-mediated resistance can be effective at controlling disease but often breaks down when pathogen effector genes mutate. In contrast, quantitative disease resistance (QDR)—also known as partial resistance—presents a continuous distribution of phenotypes from susceptible to resistant.

QDR has great potential for crop improvement due to its broad-spectrum and durable nature; however, it is not but is not frequently targeted in breeding efforts due to a lack of insights into its underlying molecular determinants (Roux *et al.*, 2014; Nelson *et al.*, 2018). QDR is generally conferred by multiple genes, limiting the ability of pathogens to evolve resistance. QDR is likely broad-spectrum as it is often associated with constitutive features that affect the growth of diverse pathogens such as host plant morphology, basal defense, and signal transduction (Raman *et al.,* 2020, Amas *et al.,* 2021, Pliet-Nayel *et al.,* 2017). Constitutive QDR may also function in combination with pathogen-specific resistance to prolong the effectiveness of *R*-genes (Pilet-Nayel *et al.,* 2017, Brun *et al.,* 2010). Although few QDR genes have been cloned and functionally validated, reported mechanisms include enhanced cell wall synthesis (Wisser *et al.*, 2005; Corwin *et al.*, 2016), enhanced secondary metabolism (Benson *et al.*, 2015) modified transport processes (Moore *et al.*, 2015; Deppe *et al.*, 2018) hormone synthesis and transcriptional regulation (Qasim *et al.,* 2020).

Identifying loci involved in broad-spectrum QDR to multiple pathogens is challenging. Different pathogens employ distinct infection and feeding strategies,

including feeding on living host cells (biotrophy); killing plant cells to feed on their contents (necrotrophy); and keeping cells alive while establishing infection before switching to a necrotrophic mode (hemibiotrophy) (Kemen and Jones, 2012). These diverse strategies necessitate differing plant defense mechanisms for effective resistance. For example, reactive oxygen species (ROS) production and cell death can provide resistance to biotrophic and hemibiotrophic pathogens (Jia *et al.,* 2000; Vleeshouwers *et al.,* 2000, Vetter *et al.,* 2012). However, ROS accumulation and cell death can promote pathogenicity for some necrotrophic pathogens that use necrosis to facilitate their colonization (Tiedemann, 1997; Govrin and Levine, 2000; Lorang *et al.,* 2007; Williams et al., 2011, Faris and Friesen, 2020). Additionally, certain plant hormones salicylic acid (SA) and jasmonic acid (JA) exhibit opposing effects on resistance dependent on pathogen lifestyle (Navarro, *et al.,* 2008): the activation of the JA-signaling provides resistance against necrotrophic pathogens; but the activation of SA-signaling protects against biotrophic and hemibiotrophic pathogens (Glazebrook, 2005).

Certain broad-spectrum QDR mechanisms could relate to innate immunity based on the detection of shared pathogenic features irrespective of their lifestyle. For example, some quantitative trait loci (QTLs) implicated in QDR resemble cell surface pattern recognition receptors (PRRs) or receptor-like kinases (RLKs), akin to those in pathogen-associated molecular pattern (PAMP)-triggered immunity (PTI) (Wisser *et al.,* 2005; Lacombe *et al.,* 2005; Schweizer and Stein, 2011; Hurni *et al.,* 2015; Schoonbeek *et al.,* 2015; Nelson *et al.,* 2018). PRRs like CHITIN ELICITOR RECEPTOR-LIKE KINASE 1 (CERK1), FLAGELLIN SENSING 2 (FLS2), and EF-TU RECEPTOR (EFR) detect PAMPs such as chitin, flg22, and elf18 respectively (Miya *et al.,* 2007; Gómez-Gómez and Boller, 2000; Zipfel *et al.,* 2006). Upon PAMP recognition, plants rapidly produce ROS like H_2O_2, followed by mitogen-activated protein kinase (MAPK) activation and defense gene induction. Measurement of ROS production by purified PAMPs has been used extensively in various laboratories to provide consistent and reliable PTI assessment and to study the relationship between PTI response and QDR (Vetter *et al.,* 2012, Samira *et al.,* 2020).

We aimed to identify broad-spectrum QDR loci in oilseed rape (*Brassica napus*) using a common panel of genotypes. *Brassica napus* is a major crop worldwide,

producing edible oil, biodiesel, and animal feed protein. Disease susceptibility significantly impacts *B. napus* yields so enhanced resistance is a major breeding objective. Employing associative transcriptomics (AT) (Harper *et al.,* 2012; Havlickova *et al.,* 2018), we previously identified single nucleotide polymorphism (SNP) and gene expression marker (GEM) candidate loci linked to *B. napus* QDR against *Pyrenopeziza brassicae* (Fell et al., 2022). The GEM analysis utilizes transcriptomic data representing a baseline pre-infection expression level—a foundation for investigating constitutive QDR. The AT pipeline has been successfully applied to diverse phenotypes including pathogen resistance, flowering time, and seed glucosinolate content (Harper *et al.,* 2012, Woodhouse *et al.,* 2021, Dakouri *et al.,* 2021; Roy *et al.,* 2021). However, to our knowledge, AT has never been used to research the similarities and differences between the loci underlying resistance to multiple pathogens.

Three hypotheses underlie our study. Firstly, using a diverse *B. napus* panel—comprising a range of crop types including winter, semi-winter, and spring oilseed rape, swede, and kale, resulting in 219k SNP variants across the genome—we hypothesized there would be variable pathogen resistance within the population due to the high level of genetic and morphological variation. This variation might correlate with constitutive defenses or early innate immunity since PAMP recognition is conserved across pathogens. Therefore, our second hypothesis is that shared QDR loci may be associated with resistance to multiple pathogens, including those with contrasting lifestyles. Finally, given pathogens of different lifestyles utilize different mechanisms for their infection, our third hypothesis is that there would be some QDR loci dependent on the lifestyle of the pathogen. To test these hypotheses, we examined resistance to two necrotrophs, *Alternaria brassicicola* and *Botrytis cinerea,* and two hemibiotrophs, *P. brassicae,* and *Verticillium longisporum*, within the diversity panel. We used AT to identify the associated loci that define the “host genetic signature” of QDR in *B. napus*. Additionally, we explored the presence of loci associated with both QDR and PTI (measured by the production of PAMP-induced ROS).

For the first time, we demonstrate that AT analyses from several pathogens can be combined to identify candidate loci for broad-spectrum QDR. We identify GEMs associated with either resistance or susceptibility dependent on the

pathogen lifestyle. Additionally, we identify a potential deletion associated with resistance to *V. longisporum* and potentially broad-spectrum QDR. This study provides new insight into the commonalities underlying broad-spectrum QDR and provides a resource for further mechanistic exploration and improving broad-spectrum resistance to pathogens in *B. napus.*

Materials and Methods

Pathogen infection assays

We selected a subset of the 191 *B. napus* genotypes for phenotyping, ensuring feasible pathology assays with ample replication across all participating labs. To mitigate environmental effects during seed production, all genotypes were cultivated under consistent environmental conditions before distribution to labs. Nevertheless, in some pathosystems, certain lines yielded unreliable data, leading to variable numbers of genotypes used for analyses.

Alternaria brassicicola

151 *B. napus* accessions were grown in peat soil (pH 5.6 – 6.8) with 1/30 Perlite, 16 h day/8 h night photoperiod under fluorescent light (Super TLD Philips 865, 100 µmol m^{-2} s^{-1}), 19°C ± 2°C and approximately 70% relative humidity. The wild-type *A. brassicicola* strain (ATCC 96836) was cultured and previously described (Macioszek *et al.,* 2018). A conidial suspension diluted to $3.5x10^5$ conidia ml^{-1} in distilled water was applied in two 10 µl drops to the third leaf of five-week-old plants. Necrotic areas were measured in three replicates per genotype at 5 days post-inoculation using WinDIAS_3 Imaging Analysis System (Delta-T Devices, UK). The experiment was repeated twice.

Botrytis cinerea

We divided 190 *B. napus* accessions into four batches for screening. Plants were grown in Levington F2 compost with 15% 4mm grit in growth chambers for 6-7 weeks under TL-tubes with a near-sunlight spectrum of 100 µmol m^{-2} s^{-1} with a photoperiod of 10 h. Temperatures were 20-22 °C/18-20 °C day/night. *Botrytis cinerea* strain B05.10 (Schoonbeek *et al.,* 2001) was grown as described previously (Stefanato *et al.*, 2009) and used for inoculations as described (Lloyd *et al.*, 2014). Spore suspensions (200 µl at 2.5×10^6 spores ml^{-1}) were spread on 1/10 PDA (2.5 g l^{-1} potato dextrose broth, 12 g l^{-1} agar), and after 24 h at 21°C, 4 mm agar plugs were used for *B. napus* inoculations of 22 mm leaf discs on 0.6% water agar. Lesion diameter of 16 replicates per genotype was measured after 48 h at 21 °C, 85-100% relative humidity, and low light (10-20 µmol m^{-2} s^{-1}). Two full experimental repeats were conducted.

Pyrenopeziza brassicae

The *P. brassicae* methods and phenotype dataset used were the same as in our previous publication (Fell *et al.*, 2022). Disease severity was scored on a scale of 1 to 6—with a score of 1 for no sporulation and 6 for the most sporulation—and was calculated for the 129 genotypes.

Verticillium longisporum

We divided 191 *B. napus* accessions into four batches for screening. Six reference lines (Falcon, SEM, Zhongyou, Loras) were used for normalization. Each line had 20 plants for both mock and *V. longisporum* inoculation. The preparation of fungal inoculum and disease assessment was done as described previously (Zheng, 2018; Zheng *et al.,* 2019). Ten-day-old conidial suspension of *V. longisporum* isolate VL43 obtained from a diseased *B. napus* plant (Zeise and Tiedemann, 2001) was used for inoculation. Ten-day-old plants with unfolded cotyledons were inoculated with water or $1x10^6$ CFU ml^{-1} spore suspension for 50 minutes. Plants were kept in a climate chamber with a 16-hour photoperiod and 22 ± 2°C temperature. Stem disease severity ranging from 1 (healthy) to 9 (dead) was assessed at 7, 14, 21, and 28 days post-inoculation. The area under the disease progress curve was calculated and normalized against reference lines.

ROS assays

190 B. napus accessions were split into four groups and cultivated in Levington F2 compost with 15% 4 mm grit in growth chambers. A near-sunlight spectrum at around 100 µmol m-2 s-1 and a 10-hour photoperiod were maintained, with temperatures of 20-22°C/18-20°C day/night. ROS measurements employed a luminol/peroxidase-based assay. For each accession, two 4 mm diameter leaf discs were taken from the second most recently expanded leaf of four individual plants, incubated in 200 µl sterile water in a 96-well plate for 16-24 hours in darkness. Subsequently, water was removed and a solution was added containing 34 mg l-1 luminol, 20 mg l-1 horseradish peroxidase (HRP), and PAMP: either chitin (100 g l-1, NA-COS-Y, Yaizu Suisankagaku Industry CO, YSK, Yaizu, Japan); flg22 (QRLSTGSRINSAKDDAAGLQIA) or elf18 (SKEKFERTKPHVNVGTIG, both 10 mM, Peptron, http://www.peptron.co.kr).

Luminescence was recorded over 40 minutes, and the total ROS response was quantified using area under the curve calculations. Two replicate experiments were conducted.

Phenotypic data transformation for association analysis

To maximize statistical power, all disease phenotype data per pathogen and *B. napus* cultivar were included (Table **S1**). Each dataset (infection phenotypes for *A. brassicicola, B. cinerea, P. brassicae,* or *V. longisporum,* ROS measurements for chitin, flg22, or elf18) was analyzed using a linear fixed- and random effects model with *B. napus* genotype as a fixed effect and experimental replicate and batch as random effects. Estimated marginal means were calculated for each *B. napus* genotype using emmeans (version 1.8.0) (R package) (R Core Team, 2023). These values were used for input into the AT pipeline. For combined data visualization, estimated marginal means were normalized to a 0-1 range. In pathogen datasets, the reciprocal of these values was used to represent 'resistance'.

Associative transcriptomics

We used genotype (SNP) and expression level datasets (Havlickova *et al.*, 2018), from York Knowledgebase (http://yorknowledgebase.info) and refined to include only the lines used within this study. Functional genotypes were determined via 100-base mRNAseq for the third true leaf using the Illumina HiSeq 2000 platform. Sequence reads were mapped to the CDS gene model-based Brassica AC pan-transcriptome reference (He *et al.,* 2015), which comprised 116,098 gene models for SNP scoring and read quantification. 219,454 SNPs with maternal allele frequencies greater than 5% were used for downstream analysis. Genome-Wide Association (GWA) and GEM mapping were done using the R-based GWA and GEM Automation (GAGA) pipeline (Nichols, 2022), which utilizes GAPIT Version 3 (Lipka *et al.*, 2012; Wang and Zhang, 2021). GAGA was run using our recently updated population structure (Fell *et al.*, 2022) and *B. napus* Pantranscriptome version 11 (Havlickova *et al.*, 2018). For GWA analyses, generalized linear model (GLM), Bayesian-information and Linkage-disequilibrium Iteratively Nested

Keyway (BLINK) (Huang *et al.,* 2019), and Fixed and random model Circulating Probability Unification (FarmCPU) (Liu *et al.,* 2016) models were compared using QQ plots to select the best-fitting model.

GEM association analyses were performed within the GAGA pipeline based on methodology by Harper *et al.* (2012). Associations were determined by linear regression using Reads Per Kilobase of the transcript, per Million mapped reads (RPKM) to predict a quantitative outcome of the trait value. Markers with an average expression below 0.5 RPKM were excluded prior to analysis resulting in 53,883 expression values for association analysis. The Pearson coefficient was utilized to assess the correlation between expression and resistance phenotype for each GEM.

To determine the statistical significance threshold in GWA analysis, various methods that account for multiple testing have been proposed, including the Bonferroni correction, Sidak correction, and False Discovery Rate (FDR). Due to the prevalence of linked markers in modern GWA, the Bonferroni correction threshold can often have an inflated significance level, detecting only strong, major gene effects as significant. To address this, we utilized the FDR to manage the expected proportion of false positives among significant associations. FDR values for both GEM and GWA were determined using the q-value R package (Storey, 2011). Bonferroni thresholds for GWA and GEM are 6.64 and 6.03-$Log_{10}P$ respectively ($P<0.05$) and 6.34 and 5.73 -$Log_{10}P$ ($P<0.1$).

Linkage disequilibrium (LD) varies based on chromosome position and selection level. To ascertain the LD at the A09 locus associated with *V. longisporum* resistance, we calculated the mean pairwise R^2 between this marker and all others on the chromosome using TASSEL Version 5.0 site by all analysis option (Bradbury *et al.,* 2007). Markers were deemed in LD when $R^2 > 0.2$.

Interpretation of data post-AT

We identified potential *Arabidopsis thaliana* orthologs of *B. napus* genes using BLASTN analysis against the *A. thaliana* transcriptome (TAIR version 10). Hypergeometric probability was used for to determine if the number of

overlapping GEMs observed was greater than that expected by chance as detailed by Kim *et al.* (2001).

We conducted weighted gene co-expression analysis (WGCNA) using the R-based WGCNA library (v 1.72) (Langfelder and Horvath, 2008). Low expressed genes with 0 RPKM value in half of the samples were removed and rest of the data was used to perform a signed WGCNA analysis to detect modules of genes using the blockwiseModules() function. A soft threshold power of 6 was selected based on minimum mean connectivity using the pickSoftThreshold() function within the WGCNA package. Correlation and p-values with phenotypic trait data were calculated using the "Cor()" and "CorPvalueStudent()" functions. Gene Ontology (GO) enrichment analysis (FDR < 0.05) was conducted using a Fisher´s exact test for GEMs within WCGNA modules.

Results

QDR to *A. brassicicola, B. cinerea, P. brassicae* and *V. longisporum* is present in the *B. napus* diversity panel

Given the extensive genetic diversity in our *B. napus* panel we hypothesized that QDR to *A. brassicicola, B. cinerea, P. brassicae,* and *V. longisporum* would be present. We did pathogenicity assays and found that the *B. napus* genotypes demonstrated varying levels of resistance to the pathogens, confirming the presence of QDR in the panel (Fig. **1a**, Table **S1**).

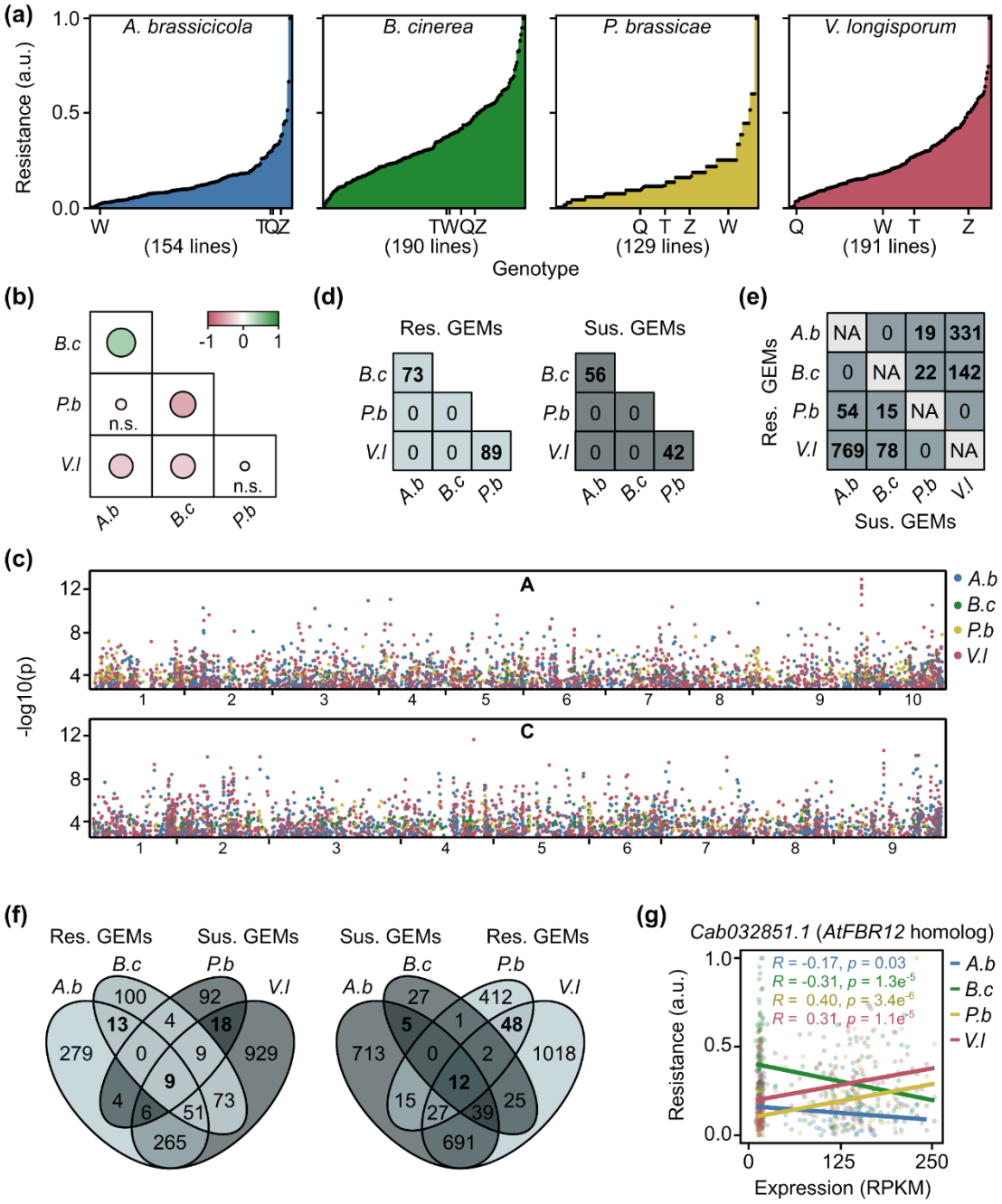

Fig. 1 *Brassica napus* genotypes have common GEMs associated with resistance pathogens of the same lifestyle. (a) *B. napus* disease resistance to fungal pathogens is quantitative. Resistance phenotype (arbitrary units (a.u.), normalized values between zero and one) of different *B. napus* genotypes to *Alternaria brassicicola* (*A.b*), *Botrytis cinerea* (*Bc*), *Pyrenopeziza brassicae* (*Pb*) or *Verticillium longisporum* (*Vl*). The total number of genotypes used for each pathogen assay and the position of reference genotypes Quinta (Q), Tapidor (T), Westar (W) and Zhongshuang 11 (Z) are indicated. (**b**) Correlation between the resistance phenotype of *B. napus* lines to the fungal pathogens. Positive correlations (green), negative correlations (red) and no correlation (n.s.); strengths of correlation (sizes of circles) are indicated between pair-wise comparisons of resistance responses. (**c**) Manhattan plot of *B/ napus* genome showing marker-trait association of statistically significant GEMs for resistance to each fungal pathogen. The x-axis indicates GEM location along the chromosome; the y-axis indicates the $-\log_{10}(p)$ (*P* value). (**d**) The numbers of resistance and susceptibility gene expression markers (GEMs) shared between pair-wise comparisons of pathogens. (**e**) The numbers of GEMs associated with resistance to one pathogen and susceptibility to another pathogen. (**f**) Venn diagrams showing the overlap between *A.b and B.c* susceptibility GEMs and *P.b* and *V.l* resistance GEMs (right) and the overlap between *A.b and B.c* resistance GEMs and *P.b* and *V.l* susceptibility GEMs (left). (**g**) Linear regression analysis of gene expression (RPKM) of *Cab032851.1* relative to resistance to fungal pathogens (arbitrary units (a.u.), normalized values between zero and one).

We hypothesized that if broad-spectrum QDR was present, there would be a positive correlation between phenotypic responses to pathogens. We initially examined disease resistance in four *B. napus* genotypes with published reference genomes: Quinta, Tapidor, Westar, and Zhongshuang 11. Quinta showed low resistance to both hemibiotrophic pathogens, while Zhongshuang 11 displayed high resistance to both necrotrophic pathogens (**Fig. 1a**). However, the ranking of these reference genotypes within the diversity panel varied. To explore correlations across the entire *B. napus* panel's responses to pathogens, we generated a correlation matrix for pairwise fungal pathogen comparisons (**Fig. 1b**). There was a positive correlation between resistance to necrotrophic pathogens *A. brassicicola* and *B. cinerea*. Conversely, negative correlations emerged between resistance to different pathogen lifestyles; for example, hemibiotrophic *V. longisporum* showed negative correlations with necrotrophic pathogens *A. brassicicola* and *B. cinerea*.

GEMs are associated with resistance to pathogens of the same lifestyle.

To identify QDR loci, we performed GWA analysis on our datasets from the four fungal pathogens. Minor GWA association peaks could be observed ($-Log_{10}P>5$) however we did not identify any significant marker associations with resistance to any of the pathogens, using either a Bonferroni threshold of P=0.1 or a false discovery rate (FDR) of 0.05. All association data provided is within Table **S2**. We performed GEM analyses using the transcriptomes of the *B. napus* genotypes to associate resistance with the expression of all gene models (Table **S3**). Numerous GEMs showed significant associations with fungal pathogen resistance (FDR < 0.05), and these were distributed evenly across the *B. napus* genome (**Fig. 1c**): 2129 GEMs for *A. brassicicola*, 370 for *B. cinerea*, 659 for *P. brassicae*, and 3222 for *V. longisporum*. We classified GEMs based on their positive or negative correlation with resistance or susceptibility, naming them 'resistance GEMs' or 'susceptibility GEMs,' respectively (**Table 1**).

Table 1. The number of gene expression markers (GEMs) associated with resistance to *Brassica napus* fungal pathogens *Alternaria brassicicola, Botrytis cinerea, Pyrenopeziza brassicae and Verticillium longisporum.* The total numbers of GEMs, GEMs with expression positively correlated with resistance (R, resistance) and negatively correlated with resistance (S, susceptibility) are indicated.

	Number of GEMs (FDR < 0.05)		
Pathogen	**Total**	R	S
A. brassicicola	2129	627	1502
B. cinerea	370	259	111
P. brassicae	659	517	142
V. longisporum	3222	1862	1360

We hypothesized that there might be shared QDR GEMs associated with all four fungal pathogens. To investigate this, we compared the lists of resistance and susceptibility GEMs across the fungal pathogens (**Fig. 1d**). While necrotrophic pathogens (*A. brassicicola* and *B. cinerea*) had shared GEMs, as did hemibiotrophic pathogens (*P. brassicae* and V. *longisporum*), there were no common GEMs between necrotrophic and hemibiotrophic pathogens. Consequently, there were no shared GEMs associated with broad-spectrum resistance spanning pathogens with differing lifestyles.

Given the existence of shared QDR GEMs associated with pathogens of the same lifestyle and that pathogens with similar lifestyles have similarities related to their infection, feeding strategies, and plant processes required for defense, we conducted overrepresentation analyses to compare the number of shared QDR GEMs between pathogens of the same lifestyle against what would be expected by chance (Plaisier *et al.,* 2010). There was significant overrepresentation in the number of shared GEMs between necrotrophic pathogens *A. brassicicola* and *B. cinerea* (73 resistance GEMs and 56 susceptibility GEMs), as well as between hemibiotrophic pathogens *P. brassicae* and *V. longisporum* (89 resistance GEMs and 42 susceptibility GEMs) (**Fig. 1d, Table S4, S5**).

GEMs are associated antagonistically with resistance to pathogens of different lifestyles.

Hemibiotrophic and necrotrophic pathogens employ distinct plant mechanisms for their infection, with certain genes that confer resistance to hemibiotrophic pathogens leading to susceptibility against necrotrophic pathogens (Lorang *et al.,* 2007). Thus, we hypothesized the presence of QDR GEMs with antagonistic associations based on pathogen lifestyle. To explore this, we compared resistance GEMs with susceptibility GEMs for each combination of fungal pathogens (**Fig. 1e**). As anticipated, we identified no GEMs with antagonistic effects for pairs of either necrotrophic or hemibiotrophic pathogens. However, intriguingly, we observed an overrepresentation of GEMs with antagonistic resistance associations between necrotrophic and hemibiotrophic pathogens. For instance, 1100 (769 + 331) GEMs with opposite resistance associations were linked to *A. brassicicola* and *V. longisporum* (**Table S4, S5**).

Broad-spectrum resistance GEMs with no antagonistic effects on susceptibility to other pathogens hold promise for crop breeding. To identify such candidates, we compared necrotrophic pathogen susceptibility GEMs to hemibiotrophic pathogen resistance GEMs. Similarly, we compared necrotrophic pathogen resistance GEMs to hemibiotrophic pathogen susceptibility GEMs (**Fig. 1f, Table S4**). 13 GEMs were associated with resistance to both *A. brassicicola* and *B. cinerea* with no associations with susceptibility to *P. brassicae* and *V.*

longisporum (Table **2**). 48 GEMs were associated with resistance to both *P. brassicae* and *V. longisporum* with no associations with susceptibility to *A. brassicicola* and *B. cinerea* (Table **3**). Notably, four GEMs homologous to *A. thaliana ACIP1* were associated with resistance to both hemibiotrophic pathogens and no antagonistic associations with susceptibility to the necrotrophic pathogens.

Interestingly, there was a significant overrepresentation of GEMs associated with susceptibility or resistance to both necrotrophic pathogens, but with opposing associations to both hemibiotrophic pathogens: 21 GEMs (9 + 12) (Table **4**, S6). Notably, the expression of *Cab032821.1*, the homolog of *A. thaliana Fumosin B1-resistant 12, FBR12*, was associated with resistance to both hemibiotrophic pathogens but susceptibility to both necrotrophic pathogens (Fig. **1g**), as was the *Bo8g081460.1,* the homolog of an *A. thaliana disease resistance nucleotide-binding leucine-rich repeat (NBS-LRR)* protein (Table **4**).

Table 2. Broad-spectrum GEMs associated with resistance (R) or susceptibility (S) to necrotrophic fungi (necro.) *Alternaria brassicicola* and *Botrytis cinerea,* with no antagonistic effects on hemibiotrophic fungi (hemi.) *Pyrenopeziza brassicae* and *Verticillium longisporum.* The putative *Arabidopsis thaliana* (*At*) orthologs, protein class, and gene ID are indicated.

GEM	Necro.	Hemi.	*At* ortholog	Gene name	Protein class
Cab019641.1	R	-	-	-	-
Cab029666.1	R	-	AT1G04980.1	*PDI10; Protein disulfide-isomerase like 2-2*	chaperone
Cab006731.1	R	-	-	-	-
Cab023848.3	R	-	AT3G13772.1	*TMN7; Transmembrane 9 superfamily member 7*	transporter
Bo6rg071140.1	R	-	AT3G56460.1	*GroES-like zinc-binding alcohol dehydrogenase family protein*	oxidoreductase
Cab006719.1	R	-	AT5G24630.5	*BIN4; Brassinosteroid insensitive 4*	DNA-binding
Bo3g028280.1	R	-	AT4G38220.2	*AQI, Aquaporin interactor, N-acyl-L-amino-acid amidohydrolase*	-
Bo9g183340.1	R	-	AT5G02820.1	*BIN5, Brassinosteroid insensitive 5, DNA topoisomerase 6 subunit A*	endodeoxyribonuclease
Bo3g004890.1	R	-	AT5G08380.1	*AGAL1; Alpha-galactosidase 1*	galactosidase
Cab010087.2	R	-	-	-	-
Cab023861.2	R	-	AT1G72730.1	*Eukaryotic initiation factor 4A-3*	RNA helicase
BnaC03g41840D	R	-	-	-	-
Bo1g017790.1	R	-	AT4G17720.1	*BPL1; Putative RRM-containing protein*	RNA splicing factor
Cab007046.1	S	-	AT5G48590.1		
Bo5g132170.1	S	-	AT3G13740.1	*RNC4; RNase III-like enzyme*	
Cab029917.1	S	-	AT1G01090.1	*PDH-E1 ALPHA; Pyruvate dehydrogenase E1 subunit alpha-3*	dehydrogenase
Bo3g040470.1	S	-	AT2G27510.1	*FD3; Ferredoxin-3*	reductase
Bo5g132390.1	S	-	AT3G13550.1	*COP10, Constitutive photomorphogenesis protein 10*	ubiquitin-protein ligase

Table 3. Broad-spectrum GEMs associated with resistance (R) or susceptibility (S) to hemibiotrophic fungi (hemi.) *Pyrenopeziza brassicae* and *Verticillium longisporum,* with no antagonistic effects on necrotrophic fungi (necro.) *Alternaria brassicicola* and *Botrytis cinerea.* The putative *Arabidopsis thaliana* (*At*) orthologs, protein class, and gene ID are indicated. Multiple GEMs corresponding to *A. thaliana* ortholog AT3G09980.1 are highlighted.

GEM	Necro.	Hemi.	*At* ortholog	Gene name	Protein class
BnaC09g43580D	-	R	-	-	-
Cab025354.2	-	R	AT2G45580.1	*CYP76C3; Cytochrome P450, family 76, subfamily C, polypeptide 3*	-
Bo4g182630.1	-	R	AT2G34470.1	*UREG; Urease accessory protein G*	-
Bo5g058580.1	**-**	**R**	**AT3G09980.1**	***ACIP1; Acetylated interacting protein 1***	**-**
Bo4g183100.1	-	R	AT2G35190.1	*NPSN11; Novel plant SNARE 11*	SNARE protein
Bo2g095510.1	-	R	AT1G80930.1	*Pre-mRNA splicing factor CWC22 homolog*	RNA processing factor
Bo9g176470.1	-	R	AT5G06250.2	*NGAL3; NGATHA-like protein 3, B3 domain-containing protein*	transcription factor
BnaC03g64760D	**-**	**R**	**AT3G09980.1**	***ACIP1; Acetylated interacting protein 1***	**-**
Cab042580.1	-	R	AT4G02710.1	*NET1C; Protein NETWORKED 1C, Ki-se interacting (KIP1-like)*	-
Bo4g045470.1	-	R	AT2G32860.1	*BGLU33; beta glucosidase 33*	-
Bo4g182440.1	-	R	AT2G34250.2	*SecY/Sec61-alpha family member protein*	transporter
Cab042707.1	-	R	AT5G51120.1	*PAMN1; Polyadenylate-binding protein 1 homolog*	translation initiation factor
Cab037277.2	-	R	AT3G22550.1	*FLZ8; FCS-Like Zinc finger 8*	-
Bo4g183310.1	-	R	AT2G35510.1	*SRO1, Similar to RCD 1, I-ctive poly [ADP-ribose] polymerase*	-
Cab025625.4	-	R	-	-	-
Bo6rg103690.1	-	R	AT1G67280.2	*GLYI6; Lactoylglutathione lyase*	lyase
Bo4g182680.1	-	R	-	-	-
Bo2g095560.1	-	R	-	-	-
Cab029121.1	-	R	AT2G26250.1	*KCS10; 3-ketoacyl-CoA synthase 10*	-
Bo5g137820.1	**-**	**R**	**AT3G09980.1**	***ACIP1; Acetylated interacting protein 1***	-
Bo4g194830.1	-	R	AT2G44120.1	*60S ribosomal protein L7-3*	ribosomal protein
Cab013800.1	-	R	AT1G16445.1	*S-adenosyl-L-methionine-dependent methyltransferases superfamily*	methyltransferase
Bo2g095550.1	-	R	-	-	-
Bo4g182550.1	-	R	AT2G34410.2	*RWA3; Reduced wall acetylation 3 homolog*	-
Bo4g182960.1	-	R	AT2G34840.1	*epsilon2-COP; Coatomer subunit epsilon-2*	vesicle coat protein
Bo1g051850.1	-	R	AT2G31290.2	*Ubiquitin carboxyl-terminal hydrolase family protein*	-
BnaC06g39270D	-	R	-	-	-
Bo1g003050.1	-	R	AT4G40000.1	*TRM4A; S-adenosyl-L-methionine-dependent methyltransferase*	R- methyltransferase
Bo4g023900.1	-	R	AT2G44620.1	*Acyl carrier protein 1, mitochondrial*	-
Cab002494.2	-	R	AT2G30320.1	-	-
Cab007584.1	-	R	AT5G05800.2	*L10-interacting MYB domain-containing protein*	-
BnaC04g02850D	**-**	**R**	**AT3G09980.1**	***ACIP1; Acetylated interacting protein 1***	**-**
BnaC05g07480D	-	R	-	-	-
Bo5g003800.1	-	R	AT1G03365.1	*Putative E3 ubiquitin-protein ligase RF4*	-

GEM	Necro.	Hemi.	*At* ortholog	Gene name	Protein class
Cab042031.1	-	R	-	-	-
Bo4g183270.1	-	R	-	-	-
Bo4g183070.1	-	R	AT2G35050.1	*Kinase superfamily domain-containing protein*	non-receptor ser/thr kinase
Bo4g182310.1	-	R	AT2G33860.1	*ARF3/ETT; Auxin response factor 3/ETTIN*	-
Cab019919.4	-	R	AT4G31040.1	*DLDG1; Chloroplast envelope membrane protein*	-
Bo6rg003510.1	-	R	AT3G18524.1	*MSH2; DNA mismatch repair protein*	D- metabolism protein
Cab019786.1	-	R	AT4G29530.1	*THMPASE1; Thiamine phosphate phosphatase-like protein*	phosphatase
Bo4g182420.1	-	R	AT3G18430.2	*Calcium-binding EF-hand family protein*	-
Bo6rg003540.1	-	R	AT1G44790.1	*Gamma-glutamylcyclotransferase 2-3*	-
Cab007776.1	-	R	AT5G11710.1	*EPS1; Clathrin interactor EPSIN 1*	membrane trafficking
Bo4g183130.1	-	R	AT2G35230.1	*IKU1; Protein HAIKU1*	-
Bo4g143960.1	-	R	AT5G37890.1	*SI-L7; E3 ubiquitin-protein ligase SI--like 7*	ubiquitin-protein ligase
Cab007778.1	-	R	-	-	-
Bo6rg003520.1	-	R	AT1G44770.1	*elongation factor*	-
Cab019945.1	-	S	-	-	-
Cab044891.1	-	S	-	-	-
BnaA08g28590D	-	S	-	-	-
Bo6rg033210.1	-	S	AT1G55090.1	*Glutamine-dependent -D(+) synthetase*	ligase
BnaC08g18360D	-	S	-	-	-
Bo2g007540.1	-	S	AT5G07210.1	*ARR21; Putative two-component response regulator 21*	transcription factor
BnaA01g02330D	-	S	-	-	-
Cab002672.1	-	S	AT2G33810.1	*SPL3; Squamosa promotor binding protein-like 3*	DNA-binding
Cab013528.1	-	S	-	-	-
Cab034921.1	-	S	AT2G38540.1	*LP1; Non-specific lipid-transfer protein 1*	-
Cab020282.2	-	S	-	-	-
Bo7g095690.1	-	S	AT5G25830.1	*GATA12; GATA transcription factor 12*	transcription factor
BnaC08g15170D	-	S	-	-	-
Cab037036.1	-	S	-	-	-
Cab034089.1	-	S	-	-	-
Bo8g087140.1	-	S	AT3G54890.1	*LHCA1; Light-harvesting complex gene 1*	-
Bo6rg098720.1	-	S	AT1G67700.1	*HHL1; Hypersensitive to high light 1*	-
Bo5g152840.1	-	S	AT3G02150.2	*PTF1; Plastid transcription factor 1*	transcription factor

444

Table 4. Broad-spectrum GEMs associated with resistance (R) or susceptibility (S) to hemibiotrophic fungi (hemi.) *Pyrenopeziza brassicae* and *Verticillium longisporum,* with antagonistic effects on necrotrophic fungi (necro.) *Alternaria brassicicola* and *Botrytis cinerea.* The putative *Arabidopsis thaliana* (*At*) orthologs, protein class, and gene ID are indicated.

GEM	Necro.	Hemi.	*At* ortholog	Gene name	Protein class
BnaA10g08980D	R	S	AT2G34470.2	*UREG; Urease accessory protein G*	
Bo2g101920.1	R	S	AT3G10020.1	*HUP26; Hypoxia unknown protein 26*	
Cab002732.1	R	S	-	-	
Bo2g101910.1	R	S	-	-	
Bo4g021310.1	R	S	AT2G44150.1	*ASHH3; Histone-lysine N-methyltransferase*	
BnaA06g22180D	R	S	-	-	
Bo7g077710.1	R	S	AT5G47570.1	*NADH dehydrogenase ubiquinone 1 beta subcomplex subunit*	dehydrogenase
Cab031167.1	R	S	-	-	
Cab017493.1	R	S	AT5G56940.1	*Ribosomal protein S16 family protein*	ribosomal protein
Cab007887.1	S	R	AT5G13310.1	-	
Bo6rg081580.1	S	R	AT1G78420.2	*DA2; mono-ubiquitinator*	
Bo9g176310.1	S	R	AT5G06310.1	*POT1b, Protection of telomeres 1b*	DNA metabolism protein
Cab029870.1	S	R	AT1G02560.1	*CLPP5; Nuclear encoded Clp protease 5*	serine protease
Bo6rg081770.1	S	R	AT1G78170.1	*EAU1, Ethylene-responsive element binding factor-associated*	
Cab032816.1	S	R	AT1G24170.1	*LGT9, Galacturonosyltransferase-like 8*	glycosyltransferase
Cab027999.1	S	R	-	-	
Cab018896.1	S	R	AT1G76610.1	*MIZU-KUSSEI-like protein*	
Bo4g151450.1	S	R	-	-	
Bo8g081460.1	S	R	AT3G51570.1	*Disease resistance protein (TIR-NBS-LRR class)*	
Cab032851.1	S	R	AT1G26630.1	*FBR12; Fumonisin B1-resistant 12*	translation initiation factor
Bo4g149580.1	S	R	AT2G22400.1	*TRM4B, S-adenosyl-L-methionine-dependent methyltransferases*	RNA methyltransferase

We conducted WGCNA analysis to explore the co-expression patterns of GEMs in our study. Several GEMs exhibited co-expression patterns across the *B. napus* population and were organized into co-expression modules. These modules were then assessed for their association with resistance to each pathogen (**Table S6**). Notably, significantly correlated modules included 22 modules (containing a total of 1075 GEMs) for resistance to *A. brassicola*, 18 modules (containing 299 GEMs) for resistance, 34 modules (containing 575 GEMs) for *P. brassicae* resistance, and 26 modules (containing 2075 GEMs) for *V. longisporum* resistance. Interestingly, modules correlated with resistance to necrotrophic pathogens displayed susceptibility to hemibiotrophic pathogens, and vice versa, consistent with the findings from our individual GEM results.

To gain further insights, we performed GO enrichment analysis on the putative *A. thaliana* orthologs of resistance and susceptibility GEMs within each module. Particularly noteworthy was a module linked to susceptibility to necrotrophic pathogens and resistance to hemibiotrophic pathogens, enriched in genes associated with photosynthesis. This suggests that photosynthesis-related processes might exert contrasting effects on resistance based on the pathogen's lifestyle. We examined if there were any GEMs related to known pathogen-dependent pathways, specifically SA or JA signaling. We first used gene ontology to search for SA- or JA-related GEMs in our whole expression dataset (53,883 markers). No GEMs were linked to SA signaling. Markers associated with JA signaling were not enriched in our GEM analysis or WGCNA modules. This is likely because these genes are usually activated in response to pathogens rather than being constitutively expressed at the represented three-leaf stage in our expression data.

GEMs associated with both PTI and QDR are dependent on pathogen lifestyle.

We had originally hypothesized the presence of shared QDR loci associated with resistance to multiple pathogens with contrasting lifestyles possibly linked to early innate immunity due to the conserved nature of PAMP recognition. However, our comparisons of GEMs (Fig. **1d**), revealed no shared GEMs between all four pathogens. Nevertheless, previous studies have linked PTI genes to QDR (Wisser *et al.,* 2005; Schweizer and Stein, 2011; Hurni *et al.,* 2015; Nelson *et al.,*

2018). Thus, we proceeded to investigate whether any of our pathogen resistance QDR loci were related to PTI.

The *B. napus* genotypes demonstrated varying levels of PAMP-induced ROS production with all three PAMPs, suggesting quantitative traits (Fig. **2a, S1a**). Reference lines (Quinta, Tapidor, Westar, and Zhongshuang 11) had comparable rankings for flg22 and elf18 ROS responses within the panel and our correlation matrix indicated that the *B. napus* genotypes exhibited similar rankings of responses across all three PAMPs (Fig. **S2b**). Minor GWA association peaks could be observed ($-Log_{10}P>5$), with a single marker (Cab031873.1:1209:C) significantly associated with flg22-induced ROS production at a Bonferroni threshold of P=0.1. No significantly associated markers were observed at an FDR of 0.05. All marker associations are detailed in Table **S2**. We identified 184, 286, and 3251 GEMs associated with chitin-, flg22-, and elf18-induced ROS responses, respectively (Table **S3**), however, no GEMs corresponded to PRRs. There was a significant overlap between GEMs associated with the different PAMP responses. For example, out of the 184 chitin-induced ROS GEMs, 31% were shared with the flg22 response, 54% with the elf18 response, and 21% with both flg22 and elf18 responses (Table **S7,** Fig. **S1c**). These data suggest that response to PAMPs has some general genetic control and some PAMP-dependent distinct elements.

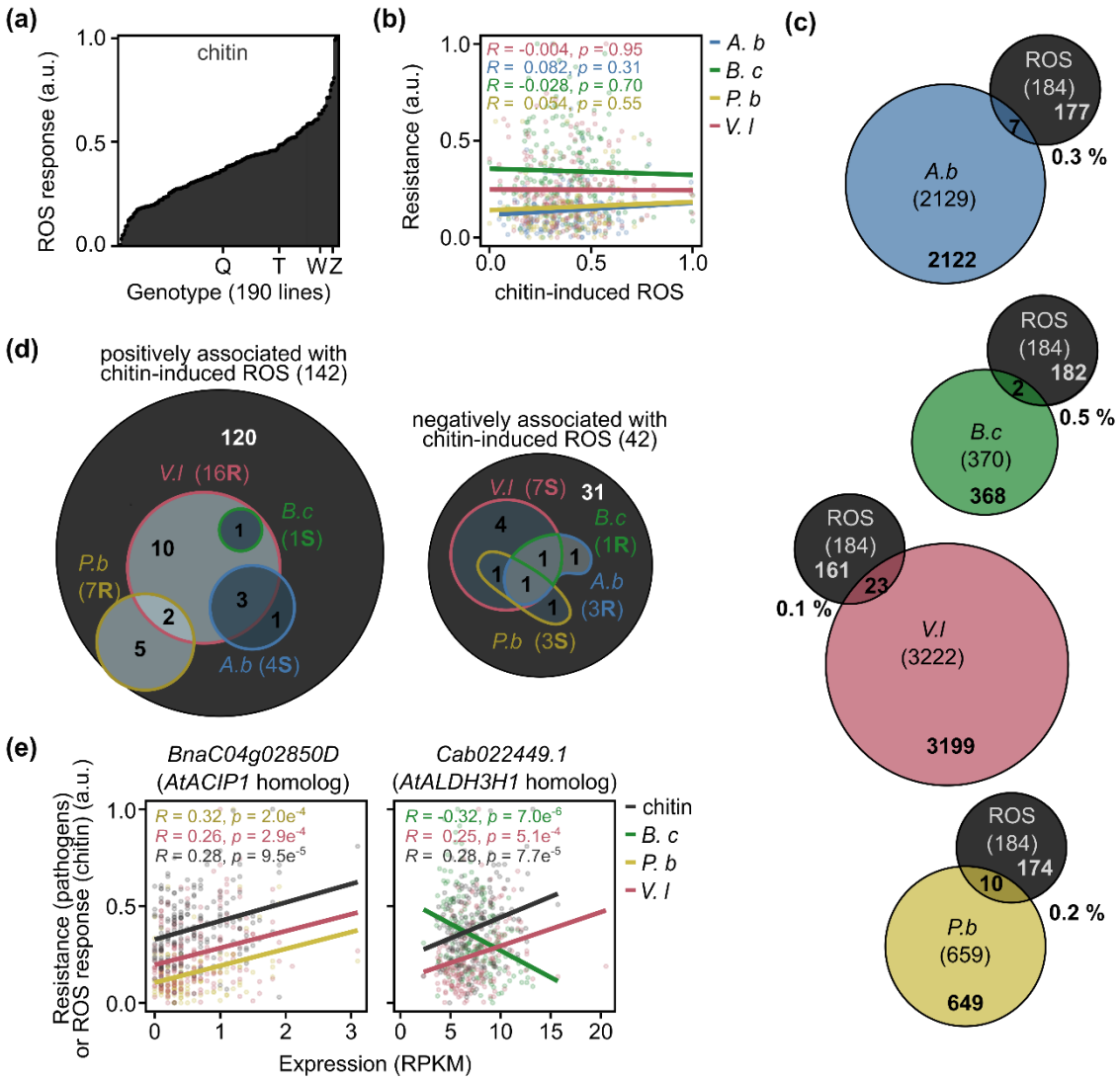

Fig. 2 Shared GEMs for QDR and chitin-induced ROS are associated with resistance to hemibiotrophic pathogens but susceptibility to necrotrophic pathogens. (**a**) Chitin-induced ROS response (arbitrary units (a.u.), normalized values between zero and one) of different *B. napus* genotypes. The positions of reference genotypes Quinta (Q), Tapidor (T), Westar (W) and Zhongshuang 11 (Z) are indicated. (**b**) Linear regression analysis of chitin-induced ROS response relative to quantitative disease resistance to *Alternaria brassicicola (A.b), Botrytis cinerea (B.c)*, *Pyrenopeziza brassicae (P.b)* or *Verticillium longisporum (V.l)* (arbitrary units (a.u.), normalized values between zero and one). (**c**) Venn diagrams showing the overlap between GEMs associated with chitin-induced ROS and QDR to the fungal pathogens, *Alternaria brassicicola* (*A.b*), *Botrytis cinerea* (*B.c*), *Pyrenopeziza brassicae* (*P.b*), and *Verticillium longisporum* (*V.l*). The percentage of QDR-related GEMs which are also related to chitin-induced ROS is indicated. (**d**) The number of gene expression markers (GEMs) whose expression was positively or negatively associated with chitin-induced ROS and the number which were also associated with resistance (R) or susceptibility (S) to the *B. napus* fungal pathogens. Venn diagram indicating the overlap between GEMs associated with several pathogen interactions. (**e**) Linear regression analysis of

gene expression (RPKM) of *BnaC04g2850D* and *Cab022449.1* relative to chitin-induced ROS responses and resistance to fungal pathogens.

Since chitin is a fungal PAMP and our study centres on fungal pathogens, we concentrated our following investigations on the overlap between chitin-associated and QDR-associated loci. Chitin-induced ROS response did not correlate with QDR to fungal pathogens (Fig. **2b**) and only a small fraction (less than 1%) of QDR GEMs for each pathogen were linked to chitin-induced ROS response (Table **S7**). Notably, there was minimal overlap between GEMs associated with chitin-induced ROS response and QDR to necrotrophic pathogens, and a slight overlap with QDR to hemibiotrophic pathogens (Table **S5**). This suggests that most QDR loci are independent of early PAMP-induced ROS response (Fig. **2c**).

Given that ROS accumulation can influence susceptibility to certain necrotrophic pathogens and our previous observation of QDR GEMs with lifestyle-dependent antagonistic associations, we investigated if loci linked to chitin-induced ROS production might be associated with resistance against hemibiotrophic pathogens but susceptibility to necrotrophic pathogens. Of the 184 GEMs that were associated with chitin-induced ROS, 142 were positively associated, i.e., increased gene expression was associated with the increased magnitude of chitin-induced ROS response. Remarkably, all chitin-induced ROS GEMs that coincided with QDR GEMs were exclusively associated with resistance to hemibiotrophic pathogens and susceptibility to necrotrophic pathogens (Fig. **2d**, Table **5**). These included *BnaC04g02850D*, a homolog of *A. thaliana ACIP1* (also associated with flg22 and elf18 responses), and *Cab022449.1*, a homolog of *A. thaliana Aldehyde dehydrogenase 3H1 (ALDH3H1)* (Table **S4**) (Fig. **2e**). Likewise, among the 42 GEMs exhibiting negative correlations with chitin-induced ROS response, those overlapping with QDR were associated with resistance against necrotrophic pathogens and susceptibility to the hemibiotrophic pathogens. WGCNA analysis revealed that GEMs linked to chitin-induced ROS were grouped into 19 modules (comprising 135 GEMs) (Table **S6**). These modules, also showed associations with modules correlated with resistance to hemibiotrophic pathogens and susceptibility to necrotrophic

pathogens, including the module enriched in GEMs related to photosynthesis regulation, aligning with our individual GEM results.

Table 5 The numbers of GEMs positively and negatively associated with chitin-induced ROS response and associated with either resistance (R) or susceptibility (S) to *Brassica napus* fungal pathogens *Alternaria brassicicola, Botrytis cinerea, Pyrenopeziza brassicae* or *Verticillium longisporum.* The direction of the correlation (positive or negative) of QDR GEMs compared to the chitin-induced ROS GEMs is also summarized.

	GEMs positively correlated with chitin-induced ROS (142)		GEMs negatively correlated with chitin-induced ROS (42)		Correlation to chitin-induced ROS GEMs
Pathogen	Number	Type (R/S)	Number	Type (R/S)	
A. brassicicola	4	S	3	R	7 -ve
B. cinerea	1	S	1	R	2 -ve
P. brassicae	7	R	3	S	10 +ve
V. longisporum	16	R	7	S	23 +ve

A 0.51 MB deletion on chromosome A09 is associated with *V. longisporum* resistance and potentially broad-spectrum QDR.

The genomic distribution of GEMs (Fig. **1c**) highlighted a notable peak of five highly significant GEMs associated with *V. longisporum* resistance on chromosome A09 (*Cab013522.1, Cab013524.1, Cab013523.1, Cab013526.1,* and *Cab013517.1*). Notably, Cab013522.1, Cab013524.1, and Cab013526.1 were also linked to *P. brassicae* resistance, while Cab013522.1, Cab013523.1, Cab013524.1, and Cab013526.1 were associated with susceptibility to *A. brassicicola* (Table **S3**). This clustering suggests a potential region of interest for broad-spectrum QDR. Compellingly, this region of chromosome A09 also corresponded to a minor association (P=5.14e^{-07}, FDR=0.11) from the *V. longisporum* resistance GWA analysis (Fig. **3a**). Assessment of phenotypic variation segregating with alleles for Cab013526.1.135.A revealed that accessions inheriting a “G” at this locus had resistance values 57% lower than those inheriting an “A” (Fig. **3b**). These alleles also segregated with resistance to *P. brassicae* (with “G” alleles showing 12% lower resistance than “A” alleles) and susceptibility to *A. brassicae* (with “G” alleles indicating 28% higher resistance than “A” alleles) (Fig. **3b**). We calculated the distance in LD with this marker and found a region of 0.51 MB containing 107 genes (Fig. **3c**).

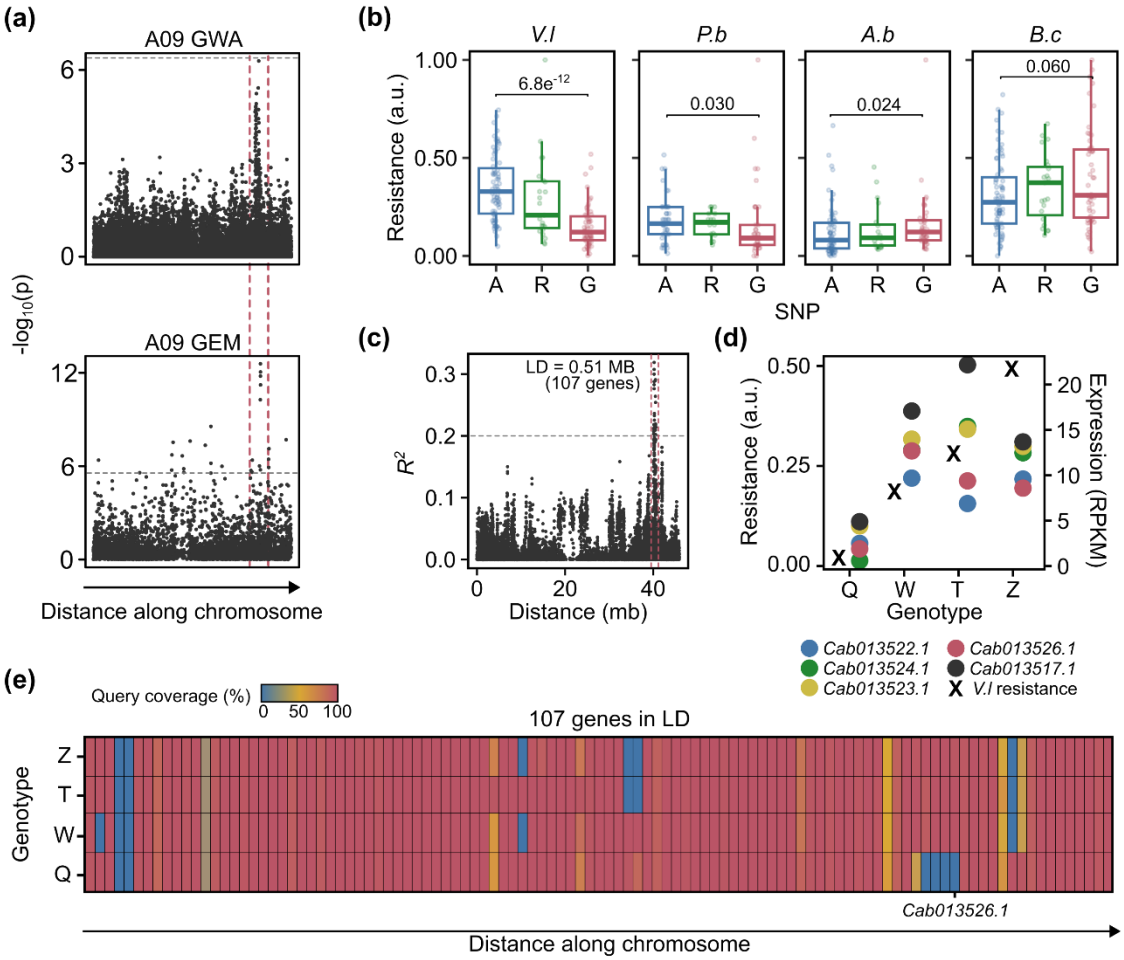

Fig. 3 Resistance *to Verticillium longisporum* is associated with a genomic deletion on chromosome A09. (**a**) Manhattan plots showing marker-trait association resulting from GEM and GWA analysis of resistance to *V. longisporum* in 191 *Brassica napus* genotypes. The x-axis indicates GEM or SNP location along the chromosome; the y-axis indicates the -$\log_{10}$(p) (*P* value). Grey line indicates the FDR > 0.05 cut-off value, red line highlights the shared region. (**b**) Segregation of resistance to *V. longisporum (V.l), Pyrenopeziza brassicae (P.b), Alternaria brassicicola (A.b),* or *Botrytis cinerea (B.c)* (arbitrary units (a.u.), normalized values between zero and one) with the highest associating marker, Cab013526.1.651.A, showing the marker effect between A and G (R = A/G). *P* values were determined by a Student's *t*-test. (**c**) Linkage decay plot from marker Cab013526.1.651.A as a function of genetic distance (MB). The grey line indicates an R^2 value of 0.2, red lines indicate the area of linkage disequilibrium. (**d**) Resistance to *V. longisporum* (left-hand y-axis) and gene expression (RPKM) of the five highest associating GEMs *Cab013522.1, Cab013524.1, Cab013523.1, Cab013526.1* and *Cab013517.1* (right-hand y-axis) in reference genotypes Quinta (Q), Tapidor (T), Westar (W) and Zhongshuang 11 (Z). (**e**) Heatmap indicating query coverage (compared to the *B. napus* pantranscriptome) in Q, T, W and Z for the 107 genes predicted to be in linkage disequilibrium with Cab013526.1.651.A on chromosome A09.

Given the association between the expression of five nearby GEMs and *V. longisporum* resistance, we speculated that this link could partly be due to a genomic deletion in this region. To explore this, we examined if any *B. napus* genotypes with published genomes (Quinta, Tapidor, Westar, and Zhongshuang 11 exhibited low gene expression and high susceptibility (Song *et al.*, 2020). Quinta had little resistance to *V. longisporum* along with low expression of the five GEMs (expression at such levels could be a result of cross-mapping to the homoeologous region on the *B. napus* 'C' genome, C08) (Fig. **3d**). On the other hand, Tapidor, Westar, and Zhongshuang 11 exhibited moderate resistance and gene expression levels. We hypothesized that Quinta has a deletion on *B. napus* chromosome A09, whereas Tapidor, Westar, and Zhongshuang 11 have not.

To determine the query coverage of the 0.51 MB region (107 genes) in LD with the most significant SNP marker, we conducted a BLAST analysis against the *B. napus* pantranscriptome for the 0.51 MB for each reference genotype. Notably, Tapidor, Westar, and Zhongshuang 11 showed nearly 100% query coverage for consecutive five genes—Cab013522.1 (40%), Cab013523.1 (0%), Cab013524.1 (0%), Cab013525.1 (0%), Cab013526.1 (0%)—while Quinta displayed reduced coverage (Table **S8**). BLAST analysis of the homoeologous region on chromosome C08 in Quinta revealed no differences compared to the other genotypes, suggesting a specific deletion on chromosome A09 (Fig. **S2a**). Linear regression analysis indicated that the expression of these five genes varied across *B. napus* genotypes and correlated with *V. longisporum* resistance (Fig. **S2b**), implying both quantitative and qualitative resistance traits associated with this region.

To identify potential genes within this deletion region that could contribute to V*. longisporum* resistance, we proposed that their homologs in the *B. napus* genome might also be relevant GEMs for resistance*.* Each of the five candidate genes on A09 only had one homolog, on chromosome C08. None of the five homologs were significant GEMs; however, linear regression analysis showed a significant association between gene expression of the *Cab013522.1* homolog (*Bo8g101810.1*) and the *Cab013524.1* homolog (Bo8g101830.1) and V. longisporum resistance (Fig. **S2b**). Downstream of the five genes, were two additional genes with nearly 100% sequence coverage in Quinta but reduced

coverage in Tapidor, Westar, and Zhongshuang 11: *BnaA09g43290D* (0%) and *Cab013532.1* (40%). However, neither of these genes was expressed during the third-leaf stage used for GEM analysis. The corresponding C08 homolog of *Cab013532.1* (*Bo8g101910.1*) also was not expressed at this stage and no C08 homolog for *BnaA09g43290D* was identified.

To infer the potential function of the five gene candidates we identified their putative *A. thaliana* orthologs using BLAST (Table **6**). The orthologs included a microtubule-binding motor protein, *Kinesin motor family protein, KIN7.2* (Cab013522.1); a carbohydrate kinase, *Xylulose kinase 1, XK1* (Cab013523.1); a multidrug and toxin extrusion (MATE) transporter, *Enhanced disease susceptibility 5 homolog, EDS5H* (Cab013524.1)*;* a plastid isoform aldolase, *Fructose-bisphosphate aldolase 1, FBA1* (Cab013525.1)*;* and a B-box zinc finger family transcription factor, *B-box domain protein 18, BBX18* (Cab013526.1)*.*

Table 6. The five genes in the deletion on chromosome A09 associated with resistance against *Verticillium longisporum*. The putative *Arabidopsis thaliana* (*At*) orthologs, protein class, and gene ID are indicated.

GEM	*At* ortholog	Gene name	Protein class
Cab013522.1	AT2G21380.1	***KIN7.2****; Kinesin motor family protein*	microtubule binding motor protein
Cab013523.1	AT2G21370.2	***XK1****, Xylulose kinase 1*	carbohydrate kinase
Cab013524.1	AT2G21340.2	***EDSH5****, Enhanced disease susceptibility 5 homolog*	transporter (MATE efflux protein)
Cab013525.1	AT2G21330.1	***FBA1****; Fructose-biphosphate aldolase 1*	aldolase
Cab013526.1	AT2G21320.1	***BBX18****; B-box domain protein 18*	zinc family transcription factor

Discussion

QDR is dependent on pathogen lifestyle.

In this study, we used an AT pipeline to investigate constitutive QDR to *B. napus* fungal pathogens: *A. brassicicola, B. cinerea, P. brassicae,* and *V. longisporum* and define the “host genetic signature” of common and unique loci associated with resistance or susceptibility.

We initially hypothesized broad-spectrum QDR across multiple pathogens with contrasting lifestyles. However, our findings revealed shared QDR loci only within similar pathogen lifestyles, either hemibiotrophic or necrotrophic. This distinction likely stems from differing infection strategies. In fact, phenotypic resistance to necrotrophic pathogens was inversely related to resistance against hemibiotrophic pathogens. This contrast was mirrored by 21 GEMs associated with broad-spectrum resistance or susceptibility to necrotrophic pathogens with an opposite association with hemibiotrophic pathogens.

Immune responses, such as cell death, can effectively counteract the endophytic growth of some pathogens like *P. brassicae* and *V. longisporum,* but necrotrophic pathogens like *A. brassicicola* and *B. cinerea* may exploit cell death mechanisms to promote their infection (McCombe *et al.*, 2022). Such contrasting effects have occasionally been previously observed, for example, an NBS-LRR gene conferring resistance to biotrophic pathogen *Puccinia coronata* f. sp. *avenae* acts as a susceptibility factor (*LOV1)* for necrotrophic pathogen *Cochliobolus victoriae* (Lorang *et al.,* 2007). Compellingly, in our study, the ortholog of a novel *A. thaliana* NBS-LRR, *Bo8g081460.1*, was associated with resistance to both hemibiotrophic pathogens and susceptibility to both necrotrophic pathogens, as was the predicted *A. thaliana* ortholog of *FBR12* which was previously shown to be involved in cell death induced by *Pseudomonas syringae* (Hopkins *et al.*, 2008).

We explored the overlap between QDR loci and PTI, and their varying associations with resistance based on pathogen lifestyle. While most QDR GEMs didn't relate to PTI, those that were positively associated with chitin-induced ROS response were associated with resistance to hemibiotrophic fungi but susceptibility to necrotrophic fungi. For instance, the *B. napus* ortholog of A.

thaliana ALDH3H1 positively correlated with chitin-induced ROS response and *V. longisporum* resistance, yet negatively correlated with resistance to *B. cinerea*. ALDH proteins—for example, a homolog of *A. thaliana* ALDH3H1, ALDH3I1—can mitigate oxidative stress by scavenging ROS (Kotchoni *et al.,* 2006). Rapid ROS production during PTI can induce programmed cell death, which can confer susceptibility to necrotrophic pathogens like *B. cinerea* (Levine *et al.,* 1994; Kotchoni and Gachomo, 2006). *B. cinerea* even produces ROS to promote its infection (Govrin and Levine, 2000) and ROS scavengers reduce infection severity (Tiedemann, 1997). Thus, it follows that genotypes with a potentially greater ability to scavenge ROS would be less susceptible to *B. cinerea*.

It's intriguing that susceptibility to necrotrophic pathogens, resistance to hemibiotrophic pathogens, and ROS production aligned with a coexpressed module enriched in GEMs linked to photosynthesis regulation. Given that ROS are generated extensively during photosynthesis, it's reasonable to suggest that some genes influencing photosynthesis could impact ROS production levels, consequently influencing resistance to necrotrophic and hemibiotrophic pathogens. Indeed, previous studies have noted distinct regulation of photosynthesis-related genes during *A. brassicicola* infection (Macioszek et al., 2020).

Identification of a narrow chromosomal region associated with broad-spectrum QDR

By combining SNP and gene expression data through AT, we identified a novel locus associated with resistance to *V. longisporum*. Further in silico analyses of the region indicated five potential candidate genes, any of which could underly the resistance phenotype. Alleles of the BBX18 homolog also segregated with resistance to *P. brassicae* and KIN7.2, EDS5H, and BBX18 homologs were GEMs for resistance to *P. brassicae,* suggesting these could be associated with broad-spectrum QDR. Although we investigated this region using reference genotype with a genomic deletion (qualitative resistance), the expression of the KIN7.2, XK1, EDS5H, FBA1, and BBX18 homologs within other genotypes in the *B. napus* population varied and was significantly associated with resistance suggesting this locus is related to QDR.

KIN7.2 is involved in microtubule-based movement and—in the animal field—kinesins have been implicated in protein trafficking for anti-fungal defense (Kurowska *et al.*, 2012; Ogbomo *et al.*, 2018). EDS5H is a homolog of EDS5, a MATE protein which functions in plant salicylic acid (SA) dependent defense (Nawrath *et al.*, 2002). However, unlike EDS5, in *A. thaliana* EDS5H is constitutively expressed in green tissues independent of pathogen infection and does not contribute to pathogen-induced SA accumulation (Parinthawong *et al.*, 2015). Nevertheless, MATE proteins transport a broad range of, such as organic acids, plant hormones, and secondary metabolites, which could influence QDR (Nawrath *et al.*, 2002; Takanashi, *et al.*, 2014; Su, *et al.,* 2022). Conversely, BBX18, as well as the additional XK1 and FBA1 genes in the potential deletion linked to resistance, lack documented defense associations.

With our in-silico analyses, we demonstrate the power of the AT pipeline to quickly narrow down on a predicted region of interest for broad-spectrum QDR. Additional functional analyses such as gene editing are needed to validate and identify the causal gene in *B. napus* and how it affects resistance to *V. longisporum* and other pathogens during infection.

Broad-spectrum QDR is an opportunity for crop breeding.

Achieving broad-spectrum disease resistance without compromising resistance to other pathogens is a crucial goal in crop breeding. For example, GEMs associated with susceptibility and no antagonistic associations with resistance could be interesting targets for gene editing to improve disease control without the introduction of transgenes (Hua *et al.*, 2019). In addition, considering crop breeding for resistance, we identified GEMs associated with resistance to both necrotrophic pathogens and no antagonistic associations with susceptibility to the hemibiotrophic pathogens. We also identified GEMs associated with resistance to both hemibiotrophic pathogens and no antagonistic associations with susceptibility to the necrotrophic pathogens including four GEMs homologous to *A. thaliana ACIP1*— ACIP1 was previously implicated in flg22-induced ROS response and resistance to *Pseudomonas syringae* (Cheong *et al.*, 2014). One of these four was positively associated with chitin-induced ROS response, highlighting it as a candidate for further investigation into its role in PTI and broad-

spectrum QDR. Future work could extend our findings to evaluate how broad the spectrum of disease control is likely to be using specific fungal strains or mutants, other *B. napus* pathogens, and different crop species.

Conclusions

Here, we used an AT pipeline to identify novel loci involved in QDR to several *B. napus* fungal pathogens *A. brassicicola, B. cinerea, P. brassicae* and *V. longisporum.* We observed broad-spectrum QDR loci were dependent on the lifestyle of the pathogen, as were associations with GEMs related to PAMP-induced ROS production. By combining GWA and GEM analyses we were able to identify a novel region of interest for *V. longisporum* resistance and potentially broad-spectrum QDR. To our knowledge, this is the first time this approach with several pathosystems has been used to identify loci involved in broad-spectrum QDR. In summary, this study provides new insight into broad-spectrum QDR and highlights interesting targets for crop breeding.

Acknowledgments

The authors thank Paweł Jedyński and Tomasz Jęcz (University of Lodz, Poland) for help with plant cultivation and inoculation with *A. brassicicola* and Aiming Qi for advice about *P. brassicae* data analysis. VKM and AKK were supported by the National Center for Research and Development, Poland (grant no. ERA-CAPS II/1/2015). XZ and AvT were supported by the German Research Foundation (grant no. ERA-CAPS DFG; TI170/13–1). HJS, RW, RB, CJR, HF, GKM, HUS and BDLF were funded by the Biotechnology and Biological Sciences Research Council (BBSRC) grants BB/N005007/1 and BB/N005112/1 (as part of the ERA-CAPS consortium “MAQBAT”). HJS, RW, CNJ, GSS, RB, and CJR were also funded by the John Innes Institute strategic program grants Plant Health BB/P012574/1 (Response BBS/E/J/000PR9796), Molecules from Nature BB/P012523/1, Genes in the Environment BB/P013511/1 and Brassica Rapeseed and Vegetable Optimisation (BRAVO) BB/P003095/1.

Competing interests

The authors declare no competing interests.

Author contributions

VKM did experiments with *A. brassicicola* infection and analysed the data with AKK. XZ did experiments and data curation with *V. longisporum* infection supervised by AvT. HF and GKM did experiments with *P. brassicae* and analysed data with HUS and HF, HUS and BDLF contributed to the conception and experimental design. RB and HJS did experiments and data curation with *B. cinerea* and PAMPs, HJS contributed to the conception and experimental design, and HJS and CNJ analysed the data. CNJ did statistical analysis of all datasets, CNJ and RW did association transcriptomics, GSS did the WGCNA analysis, and BS did the BLAST validation of the genomic deletion. CNJ, RW and CJR contributed to the conception, data interpretation and in-silico analyses post-AT. The first draft of the manuscript was written by CNJ, and all authors commented on subsequent versions of the manuscript. All authors read and approved the final manuscript.

Data availability

The R-based GAGA pipeline is available at https://github.com/bsnichols/GAGA. Our population structure is available in Fell *et al.* (2022). Supplemental files are also available at https://zenodo.org/record/8321694.

References

Amas JC, Thomas WJ, Zhang Y, Edwards D, Batley J. 2022 Key advances in the new era of genomics-assisted disease resistance improvement of *Brassica* species. *Phytopathology*: PHYTO-08-22-0289-FI

Benson JM, Poland JA, Benson BM, Stromberg EL, Nelson RJ. 2015. Resistance to gray leaf spot of maize: genetic architecture and mechanisms elucidated through nested association mapping and near-isogenic line analysis. *PLoS Genetics* **11:** e1005045.

Bradbury PJ, Zhang Z, Kroon DE, Casstevens TM, Ramdoss Y, Buckler ES. 2007. TASSEL: Software for association mapping of complex traits in diverse samples. *Bioinformatics* **23:** 2633-2635.

Brun H, Chèvre AM, Fitt BD, Powers S, Besnard AL, Ermel M, Huteau V, Marquer B, Eber F, Renard M, Andrivon D. 2010. Quantitative resistance increases the durability of qualitative resistance to Leptosphaeria maculans in Brassica napus. *New Phytologist* **185:** 285-299.

Cheong MS, Kirik A, Kim JG, Frame K, Kirik V, Mudgett, MB. 2014. AvrBsT acetylates Arabidopsis ACIP1, a protein that associates with microtubules and is required for immunity. *PLoS Pathogens,* **10:** e1003952.

Corwin JA, Copeland D, Feusier J, Subedy A, Eshbaugh R, Palmer C, Maloof J, Kliebenstein DJ. 2016. The quantitative basis of the *Arabidopsis* innate immune system to endemic pathogens depends on pathogen genetics. *PLoS Genetics* **12:** e1005789.

Corwin JA, Kliebenstein DJ. 2017. Quantitative resistance: more than just perception of a pathogen. *The Plant Cell* **29:** 655-665.

Dakouri A, Lamara M, Karim M, Wang J, Chen Q, Gossen BD, Strelkov SE, Hwang S-F, Peng G, Yu F. 2021. Identification of resistance loci against new pathotypes of *Plasmodiophora brassicae* in *Brassica napus* based on genome-wide association mapping. *Scientific Reports* **11:** 6599.

Deppe, JP, Rabbat R, Hörtensteiner S, Keller B, Martinoia E, Lopéz-Marqués RL. 2018. The wheat ABC transporter Lr34 modifies the lipid environment at the plasma membrane. *Journal of Biological Chemistry* **293:** 18667-18679.

Faris JD, Friesen TL. 2020. Plant genes hijacked by necrotrophic fungal pathogens. *Current Opinion in Plant Biology* **56**: 74-80.

Fell H, Ali AM, Wells R, Mitrousia GK, Woolfenden H, Schoonbeek H-J, Fitt BDL, Ridout CJ, Stotz H. 2022. Novel gene loci associated with susceptibility or cryptic quantitative resistance to *Pyrenopeziza brassicae* in *Brassica napus*. *Theoretical and Applied Genetics,* in press.

Ferrari S, Galletti R, Denoux C, De Lorenzo G, Ausubel FM, Dewdney J. 2007. Resistance to *Botrytis cinerea* induced in Arabidopsis by elicitors is independent of salicylic acid, ethylene, or jasmonate signaling but requires *PHYTOALEXIN DEFICIENT3 Plant Physiology* **144:** 367-379.

Fisher MC, Hawkins NJ, Sanglard D, Gurr SJ. 2018. Worldwide emergence of resistance to antifungal drugs challenges human health and food security. *Science* **360:** 739-742.

Glazebrook J. 2005. Contrasting Mechanisms of Defense Against Biotrophic and Necrotrophic Pathogens. *Annual Review of Phytopathology* 43: 205-227

Govrin EM, Levine A. 2000. The hypersensitive response facilitates plant infection by the necrotrophic pathogen *Botrytis cinerea*. *Current Biology* **10:** 751-757.

Gómez-Gómez L, Boller T. 2000. FLS2: an LRR receptor–like kinase involved in the perception of the bacterial elicitor flagellin in *Arabidopsis*. *Molecular Cell* **5**: 1003-1011.

Harper AL, Trick M, Higgins J, Fraser F, Clissold L, Wells R, Hattori C, Werner P, Bancroft I. 2012. Associative transcriptomics of traits in the polyploid crop species *Brassica napus*. *Nature Biotechnology* **30:** 798-802.

Havlickova L, He Z, Wang L, Langer S, Harper AL, Kaur H, Broadley MR, Gegas V, Bancroft I. 2018. Validation of an updated associative transcriptomics platform for the polyploid crop species *Brassica napus* by dissection of the genetic architecture of erucic acid and tocopherol isoform variation in seeds. *The Plant Journal* **93:** 181-192.

He Z, Cheng F, Li Y, Wang X, Parkin IA, Chalhoub B, Liu S, Bancroft I. 2015. Construction of Brassica A and C genome-based ordered pan-transcriptomes for use in rapeseed genomic research. *Data in Brief* 4: 357-362.

Hopkins MT, Lampi Y, Wang TW, Liu Z, Thompson JE. 2008. Eukaryotic translation initiation factor 5A is involved in pathogen-induced cell death and development of disease symptoms in Arabidopsis. *Plant Physiology* **148:** 479-489.

Hua K, Zhang J, Botella JR, Ma C, Kong F, Liu B, Zhu J-K. 2019. Perspectives on the application of genome-editing technologies in crop breeding. *Molecular Plant* **12:** 1047-1059.

Huang M, Liu X, Zhou Y, Summers RM, Zhang Z. 2019. BLINK: a package for the next level of genome-wide association studies with both individuals and markers in the millions. *Gigascience* **8:** giy154.

Hurni S, Scheuermann D, Krattinger SG, Kessel B, Wicker T, Herren G, Fitze MN, Breen J, Presterl T, Ouzunova M. 2015. The maize disease resistance gene *Htn1* against northern corn leaf blight encodes a wall-associated receptor-like kinase. *Proceedings of the National Academy of Sciences* **112:** 8780-8785.

Jia Y, McAdams SA, Bryan GT, Hershey HP, Valent B. 2000. Direct interaction of resistance gene and avirulence gene products confers rice blast resistance. *The EMBO Journal* **19:** 4004-4014.

Jones A. 2000. Does the plant mitochondrion integrate cellular stress and regulate programmed cell death? *Trends in Plant Science* **5:** 225-230.

Kemen E, Jones, JDG. 2012. Obligate biotroph parasitism: can we link genomes to lifestyles? *Trends in Plant Science* **17:** 448-457.

Kim S, Kiraly M, Jiang M, Stuart JM, Eizinger Am Wylie BN, Davidson GS. 2001. A Gene Expression Map for *Caenorhabditis elegans. Science* **5537:** 2087-2092

Kotchoni SO, Gachomo EW. 2006. The reactive oxygen species network pathways: an essential prerequisite for perception of pathogen attack and the acquired disease resistance in plants. *Journal of Biosciences* **31:** 389-404.

Kotchoni SO, Kuhns C, Ditzer A, Kirch HH, Bartels D. 2006. Over-expression of different *aldehyde dehydrogenase* genes in *Arabidopsis thaliana* confers tolerance to abiotic stress and protects plants against lipid peroxidation and oxidative stress. *Plant, Cell and Environment* **29:** 1033-1048.

Kou Y, Wang S. 2010. Broad-spectrum and durability: understanding of quantitative disease resistance. *Current Opinion in Plant Biology* **13:** 181-185.

Kurowska M, Goudin N, Nehme NT, Court M, Garin J, Fischer A, de Saint Basile G, Ménasché G. 2012. Terminal transport of lytic granules to the immune synapse is mediated by the kinesin-1/Slp3/Rab27a complex. *Blood* **119:** 3879-3889.

Lacombe S, Rougon-Cardoso A, Sherwood E, Peeters N, Dahlbeck D, van Esse HP, Smoker M, Rallapalli G, Thomma BP, Staskawicz B et al. 2010. Interfamily transfer of a plant pattern-recognition receptor confers broad-spectrum bacterial resistance. *Nature Biotechnology,* **28:** 365-369.

Laluk K, Mengiste T. 2010. Necrotroph attacks on plants: wanton destruction or covert extortion? *The Arabidopsis Book* **8:** e0136

Langfilder P, Horvath S. 2008. WGCNA: an R package for weighted correlation network analysis. *BMC Bioinformatics* **9:** 559

Levine A, Tenhaken R, Dixon R, Lamb C. 1994. H_2O_2 from the oxidative burst orchestrates the plant hypersensitive disease resistance response. *Cell* **79:** 583-593.

Lipka AE, Tian F, Wang Q, Peiffer J, Li M, Bradbury PJ, Gore MA, Buckler ES, Zhang Z. 2012. GAPIT: genome association and prediction integrated tool. *Bioinformatics* **28:** 2397-2399.

Liu X, Huang M, Fan B, Buckler ES, Zhang Z. 2016. Iterative usage of fixed and random effect models for powerful and efficient genome-wide association studies. *PLoS Genetics* **12:** e1005767.

Lloyd SR, Schoonbeek H-J, Trick M, Zipfel C, Ridout CJ. 2014. Methods to study PAMP-triggered immunity in *Brassica* species, *Molecular Plant-Microbe Interactions* **27:** 286-295.

Lorang JM, Sweat TA, Wolpert TJ. 2007. Plant disease susceptibility conferred by a “resistance” gene. *Proceedings of the National Academy of Sciences* **104:** 14861-14866.

Macioszek VK, Lawrence CB, Kononowicz AK. 2018. Infection cycle of *Alternaria brassicicola* on *Brassica oleracea* leaves under growth room conditions. *Plant Pathology* **67:** 1088-1096.

Macioszek VK, Gapińska M, Zmienko A, Sobczak M, Skoczowski A, Oliwa J, Kononowicz AK. 2020. Complexity of *Brassica oleracea–Alternaria brassicicola* susceptible interaction reveals downregulation of photosynthesis at ultrastructural, transcriptional, and physiological levels. *Cells*, **9:** 2329.

McCombe CL, Greenwood JR, Solomon PS, Williams SJ. 2022. Molecular plant immunity against biotrophic, hemibiotrophic, and necrotrophic fungi. *Essays in Biochemistry* **66:** 581-593.

McDowell JM, Woffenden BJ. 2003. Plant disease resistance genes: recent insights and potential applications. *Trends in Biotechnology* **21:** 178-183.

Miya A, Albert P, Shinya T, Desaki Y, Ichimura K, Shirasu K, Narusaka Y, Kawakami N, Kaku H, Shibuya N. 2007. CERK1, a LysM receptor kinase, is essential for chitin elicitor signaling in *Arabidopsis*. *Proceedings of the National Academy of Sciences* **104:** 19613-19618.

Moore JW, Herrera-Foessel S, Lan C, Schnippenkoetter W, Ayliffe M, Huerta-Espino J, Lillemo M, Viccars L, Milne R, Periyannan, S. 2015. A recently evolved hexose transporter variant confers resistance to multiple pathogens in wheat. *Nature Genetics* **47:** 1494-1498.

Navarro L, Bari R, Achard P, Lisón P, Nemri A, Harberd N, Jones J. 2008. DELLAs Control Plant Immune Responses by Modulating the Balance of Jasmonic Acid and Salicylic Acid Signaling. *Current Biology* **18:** 650-655.

Nawrath C, Heck S, Parinthawong N, Métraux J-P. 2002. EDS5, an essential component of salicylic acid–dependent signaling for disease resistance in Arabidopsis, is a member of the MATE transporter family. *The Plant Cell* **14:** 275-286.

Nelson R, Wiesner-Hanks T, Wisser R, Balint-Kurti P. 2018. Navigating complexity to breed disease-resistant crops. *Nature Reviews Genetics* **19:** 21-33.

Nichols B. 2022. 'A pipeline for GEM And GWAS automation', *GitHub* URL https://github.com/bsnichols/GAGA.

Ogbomo H, Timm-McCann M, Barnes T, Xiang RF, Jamil K, Ganguly A, Stack D, Huston SM, Li SS, Colarusso P. 2018. Granule-dependent NK cell killing of cryptococcus requires kinesin to reposition the cytolytic machinery for directed cytotoxicity. *Cell Reports* **24:** 3017-3032.

Parinthawong N, Cottier S, Buchala A, Nawrath C, Métraux J-P. 2015. Localization and expression of EDS5H a homologue of the SA transporter EDS5. *BMC Plant Biology* **15:** 135.

Plaisier SB, Taschereau R, Wong JA, Graeber TG. 2010. Rank–rank hypergeometric overlap: identification of statistically significant overlap between gene-expression signatures. *Nucleic Acids Research* **38:** e169.

Pilet-Nayel ML, Moury B, Caffier V, Montarry J, Kerlan MC, Fournet S, Durel CE, Delourme R. 2017. Quantitative resistance to plant pathogens in pyramiding strategies for durable crop protection. *Frontiers in Plant Science* **8**: 1838.

Qasim MU, Zhao Q, Shahid M, Samad RA, Ahmar S, Wu J, Fan C, Zhou Y. 2020. Identification of QTLs containing resistance genes for Sclerotinia stem rot in *Brassica napus* using comparative transcriptomic studies. *Frontiers in Plant Science* **11:** p.776.

R Core Team (2023). _R: A Language and Environment for Statistical Computing. R Foundation for Statistical Computing, Vienna, Austria. https://www.R-project.org/.

Raman R, Diffey S, Barbulescu DM, Coombes N, Luckett D, Salisbury P, Cowley R, Marcroft S, Raman H. 2020. Genetic and physical mapping of loci for resistance to blackleg disease in canola (*Brassica napus* L.). *Scientific Reports* **10**: 4416.

Roux F, Voisin D, Badet T, Balagué C, Barlet X, Huard-Chauveau C, Roby D, Raffaele S. 2014. Resistance to phytopathogens *e tutti quanti*: placing plant quantitative disease resistance on the map. *Molecular Plant Pathology* **15:** 427-432.

Roy J, Shaikh TM, del Río Mendoza L, Hosain S, Chapara V, Rahman M. 2021. Genome-wide association mapping and genomic prediction for adult stage sclerotinia stem rot resistance in *Brassica napus* (L) under field environments. *Scientific Reports* **11:** 21773.

Samira R, Kimball JA, Samayoa LF, Holland JB, Jamann TM, Brown PJ, Stacey G, Balint-Kurti PJ. 2020. Genome-wide association analysis of the strength of the MAMP-elicited defense response and resistance to target leaf spot in sorghum. *Scientific Reports* **10:** 20817.

Schoonbeek H-J, Del Sorbo G, De Waard MA. 2001. The ABC transporter BcatrB affects the sensitivity of *Botrytis cinerea* to the phytoalexin resveratrol and the fungicide fenpiclonil. *Molecular Plant-Microbe Interactions* **14:** 562-571.

Schoonbeek H-J, Wang HH, Stefanato FL, Craze M, Bowden S, Wallington E, Zipfel C, Ridout CJ. 2015. Arabidopsis EF-Tu receptor enhances bacterial disease resistance in transgenic wheat. *New Phytologist* **206:** 606-613.

Schweizer P, Stein N. 2011. Large-scale data integration reveals colocalization of gene functional groups with meta-QTL for multiple disease resistance in barley. *Molecular Plant-Microbe Interactions* **24:** 1492-1501.

Song J-M, Guan Z, Hu J, Guo C, Yang Z, Wang S, Liu D, Wang B, Lu S, Zhou R. 2020. Eight high-quality genomes reveal pan-genome architecture and ecotype differentiation of *Brassica napus*. *Nature Plants* **6:** 34-45.

Stefanato FL, Abou-Mansour E, Buchala A, Kretschmer M, Mosbach A, Hahn M, Bochet CG, Métraux JP, Schoonbeek H-J. 2009. The ABC transporter BcatrB from *Botrytis cinerea* exports camalexin and is a virulence factor on *Arabidopsis thaliana*. *The Plant Journal* **58:** 499-510.

Storey JD. 2011. False Discovery Rate. In: Lovric M, eds. *International Encyclopedia of Statistical Science.* Heidelberg, Berlin, Germany: Springer, 504-508.

Su Q, Rong W, Zhang Z. 2022. The pathogen-induced MATE gene *TaPIMA1* is required for defense responses to *Rhizoctonia cerealis* in wheat. *International Journal of Molecular Sciences* **23:** 3377.

Takanashi K, Shitan N, Yazaki K. 2014. The multidrug and toxic compound extrusion (MATE) family in plants. *Plant Biotechnology* **31:** 417-430.

Tiedemann AV. 1997. Evidence for a primary role of active oxygen species in induction of host cell death during infection of bean leaves with *Botrytis cinerea*. *Physiological and Molecular Plant Pathology* **50:** 151-166.

Vetter MM, Kronholm I, He F, Häweker H, Reymond M, Bergelson J, Robatzek S, de Meaux J. 2012. Flagellin perception varies quantitatively in *Arabidopsis thaliana* and its relatives. *Molecular Biology and Evolution* **29:** 1655-1667.

Vleeshouwers VGAA, van Dooijeweert W, Govers F, Kamoun S, Colon LT. 2000. The hypersensitive response is associated with host and nonhost resistance to *Phytophthora infestans*. *Planta* **210:** 853-864.

Wang J, Zhang Z. 2021. GAPIT Version 3: boosting power and accuracy for genomic association and prediction. *Genomics, Proteomics and Bioinformatics* **19:** 629-640.

Williams B, Kabbage M, Kim H-J, Britt R, Dickman MB. 2011. Tipping the balance: *Sclerotinia sclerotiorum* secreted oxalic acid suppresses host defenses by manipulating the host redox environment. *PLoS Pathogens* **7:** e1002107.

Wisser RJ, Sun Q, Hulbert SH, Kresovich S, Nelson RJ. 2005. Identification and characterization of regions of the rice genome associated with broad-spectrum, quantitative disease resistance. *Genetics* **169:** 2277-2293.

Woodhouse S, He Z, Woolfenden H, Steuernagel B, Haerty W, Bancroft I, Irwin JA, Morris RJ, Wells R. 2021. Validation of a novel associative transcriptomics pipeline in Brassica oleracea: identifying candidates for vernalisation response. *BMC genomics* **22:** 1-13.

Zeise K, Tiedemann AV. 2001. Morphological and physiological differentiation among vegetative compatibility groups of *Verticillium dahliae* in relation to *V. longisporum*. *Journal of Phytopathology* **149:** 469-475.

Zheng X. 2018. *Verticillium longisporum on oilseed rape (Brassica napus L.): differential roles of salicylic acid, seed transmission and plant colonization in greenhouse and field conditions.* PhD Thesis, Niedersächsische Staats-und Universitätsbibliothek Göttingen, Germany.

Zheng X, Koopmann B, von Tiedemann A. 2019. Role of salicylic acid and components of the phenylpropanoid pathway in basal and cultivar-related resistance of oilseed rape (*Brassica napus*) to *Verticillium longisporum*. *Plants* 8: 491.

Zipfel C, Kunze G, Chinchilla D, Caniard A, Jones JD, Boller T, Felix G. 2006. Perception of the bacterial PAMP EF-Tu by the receptor EFR restricts Agrobacterium-mediated transformation. *Cell* **125:** 749-760.

Supporting Information

Fig. S1 Comparisons between chitin-, flg22- and elf18-induced ROS responses for the phenotypes and associated gene expression markers (GEMs).

Fig. S2 Query coverage in *Brassica napus* reference genotypes and gene expression in *B. napus* population for region on chromosome C08 homoeologous to the region on A09 associated with resistance to *Verticillium longisporum*.

Table S1 Mean, normalized phenotype data for resistance to pathogens (*Alternaria brassicicola, Botrytis cinerea, Pyrenopeziza brassicae* and *Verticillium longisporum*) and ROS response induced by PAMPS (chitin, flg22, and elf18).

Table S2 Full list of single nucleotide polymorphism (SNP) markers and significance levels from genome-wide association (GWA) analyses for resistance to pathogens (*Alternaria brassicicola, Botrytis cinerea, Pyrenopeziza brassicae* and *Verticillium longisporum*) and ROS response induced by PAMPS (chitin, flg22, and elf18).

Table S3 Full list of gene expression markers (GEMs) and significance levels from GEM analyses for resistance to pathogens (*Alternaria brassicicola, Botrytis cinerea, Pyrenopeziza brassicae* and *Verticillium longisporum*) and ROS response induced by PAMPS (chitin, flg22, and elf18).

Table S4 184 gene expression markers (GEMs) associated with chitin-induced ROS compared with GEMs associated with resistance to pathogens (*Alternaria brassicicola, Botrytis cinerea, Pyrenopeziza brassicae* and *Verticillium longisporum*) and ROS response induced by flg22, and elf18. Lists correspond to Venn diagrams in Fig. 2**.**

Table S5 Enrichment analyses to determine if the number of gene expression markers (GEMs) shared between different lists is greater than the number of GEMs that would be expected by chance (e.g., lists of quantitative disease resistance (QDR) GEMs for two fungal pathogens).

Table S6 Results from Weighted Co-expression Gene Network Analysis. Significant modules, significant GEM markers within modules, and GO terms associated with the magenta and black modules are indicated.

Table S7 Shared gene expression markers (GEMs) associated with resistance to different pathogens (*Alternaria brassicicola, Botrytis cinerea, Pyrenopeziza brassicae* and *Verticillium longisporum*). Lists correspond to matrices and Venn diagrams in Fig. 1.

Table S8 List of genes in linkage disequilibrium with the top marker for *Verticillium longisporum* resistance from genome-wide association (GWA) analysis on chromosome A09, the homoeologous region on C08, and their query coverage in *Brassica napus* reference genotypes**.**